VAMOS

VAriabilité des MOuvement du Sol sur un site spécifique

Abstract

We show in this paper that source and site effects are strongly linked in the generation of ground motions, and that, even for earthquakes of the same size, the site effect depends on the details of the rupture process that will interact-or not with the site. We first propose to highlight this using a modelisation approach that uses both real and numerical data. We generate a set of 500 source time functions that accounts for the variability of the source process for a given event magnitude, and convolve then with the recordings of a small earthquake taken as an empirical Green's Function (EGF) at different stations. We have used for the EGF a Mw 4.5 even that occurred in the Guadeloupe islands (French West Indies) very well recorded by an accelerometric network. We show that the same set of source time functions generate different values of sigma at each station. We then focus our attention on two close by stations installed on different site conditions (rock and soft soil) and analyze in the time and frequency domain why the station prone to site effect generate a much larger variability for PGA than station on rock.

Introduction

To perform seismic hazard assessment of a given region, one of key step is the estimation of ground motions expected at a site from a future earthquake. To do so, most of seismic hazard studies use ground motion prediction equations (GMPEs). These relations are obtained empirically through regression analysis of databases of recorded ground motions. A GMPE allows calculating the mean value of a ground motion parameter Y (e.g. PGA, PGV, Spectral Accelerations …) as a function of magnitude M, source-to-site distance R and other variables p_i that characterize the type of faulting or local soil conditions (e.g. Reiter, 1990; Douglas, 2003).

But, beyond the estimation of a mean value, the associated standard deviation σ (commonly referred to as "sigma") also has a strong influence on computation of the probability of exceedance of a ground motion level at a site, especially for low probability levels (e.g. Bommer and Abrahamson, 2006). These low probabilities are needed for seismic hazard assessment studies at very long term and have particularly implications for the seismic design of critical facilities, such as nuclear power plants, dams and hazardous waste depository sites. The "sigma" of GMPEs has thus become the topic of increasing attention in many studies. However, as the GMPEs are developed by considering recordings from many different sites and by including multiple seismic sources, it is difficult to investigate the behavior of individual components of the random variability of ground motions. The random variability of ground motions, that represents the uncertainty due to the random nature of the processes under consideration, can be decomposed into two parts:

- the inter-event variability (denoted by τ), that represents the variability of ground motions observed at a single site for different events;
- and the intra-event variability (denoted by ϕ), that represents the variability of ground motions observed at different sites for a single event.

To better understand the nature of "sigma", recent studies (e.g. Atkinson, 2006; Morikawa *et al.,* 2008; Hiemer *et al.,* 2011; Lin *et al.*, 2011; Rodriguez-Marek *et al.*, 2011) have aimed to isolate and examine the random variability of ground motions observed at a single site for a single source of earthquakes (denoted by τ_0, c.f. Al Atik *et al.,* 2010).

The purpose of our study is to analyze the variability of ground motions that can be generated at a given site from a database of synthetic accelerograms built using an empirical Green's function simulation method. This approach enables to generate a large number of synthetic source time functions that represent simply the variability of the rupture process and to use real seismograms to take into account, in a realistic way, path and site effects, even at high frequencies. We have worked on the simulations of a M_w=6.4 earthquakes occurring on the fault at the origin of the November 21, 2004, Les Saintes earthquake (Guadeloupe, French Indies) on ten different stations of the French Permanent Accelerometric Network (Pequegnat *et al.,* 2008; see: http://www-rap.obs.ujf-grenoble.fr). A special focus will be made on the results obtained at two stations of the city of Pointe-à-Pitre, located at the same epicentral distance but on two different types of soils.

Simulation method

In order to obtain realistic synthetic accelerograms in a broad frequency range, we use a simulation method based on the Empirical Green's Function (EGF) approach (Hartzell, 1978). A small, well-recorded earthquake is chosen in the region of interest. Its recordings, taken as Empirical Green's Functions (EGFs), are combined to simulate ground motions corresponding to a larger earthquake with the same focal mechanism. We assume that the recordings of the small event represent Green's functions at each point of the fault plane activated during the rupture of the large, simulated event. This method is based on the assumption of similarity between earthquakes of different sizes, by considering that small and large earthquake are a similar phenomenon to a scale factor. Thus, the waves emitted by a small earthquake experience the same propagation effects between source and station as those issued by a larger earthquake. The EGF method therefore allows overcoming the problem of knowledge of the propagation medium, since it has the advantage of taking into account both path and site effects at different stations, which are information contained in the recordings of small earthquakes.

Among the possible EGF simulation methods, we used the stochastic two-step method developed by Kohrs-Sansorny *et al.* (2005) based on the previous works of Joyner and Boore (1986), Wennerberg (1990) and Ordaz *et al.* (1995). This method has proved its efficiency for simulating the ground motions observed during the Les Saintes earthquake (M_w=6.4), provided that a proper small event could be chosen as an EGF (Courboulex *et al.,* 2010).

The principle of the method is simple. In time domain, a large number of source time functions called Equivalent Source Time Functions (ESTFs, see Kohrs-Sansorny et al. (2005) for more precisions) are randomly generated following probability densities proposed by Ordaz *et al.* (1995). And each *ESTF(t)*, representative of a given rupture process, is

convolved with the small-event record *s(t)* taken as an EGF, to produce a large number of different synthetic accelerograms *S(t)* of the target event (Figure 1):

$$EGF(t) * ESTF(t) = S(t) \qquad (2)$$

To produce simulations consistent with the ω^{-2} model spectra (Aki, 1967; Brune, 1970) on a broad frequency range, the use of this method requires fundamental constraints on the parameters η and κ (Eq. 3 and 4). The parameter η represents the number of small earthquakes to sum together and the parameter κ is a scale factor that allows reconstructing the energy content of the target earthquake.

$$\eta = N^4 \quad \text{and} \quad \kappa = \frac{C}{N} \qquad (3), (4)$$

$$\text{where:} \quad N = \frac{f_c}{F_c}, \quad C = \frac{\Delta\Sigma}{\Delta\sigma} \quad \text{and} \quad CN^3 = \frac{M_0}{m_0} \qquad (5), (6), (7)$$

This method has the advantage of requiring only four input parameters: (1) the seismic moment M_0 of the target event; (2)(3) the seismic moment m_0 and the corner frequency f_c of the small event taken as an EGF; (4) and the ratio C between the static stress drop of the target event $\Delta\Sigma$ and that of the small event $\Delta\sigma$.

Creation of the database of synthetic accelerograms

To create the database of synthetic accelerograms needed for our study, we propose to generate a large number of different simulations of M_w=6.4 earthquakes occurring on the fault at the origin of the Les Saintes earthquake (November 21, 2004; 11h41min). The M_w=6.4 Les Saintes mainshock has occurred offshore between the Guadeloupe archipelago and the Dominica Island, ten kilometers south-east of the Les Saintes islands, with an estimated depth of 14.2 km (Bertil *et al.,* 2005). This earthquake is associated with the rupture of 13 km of a normal fault belonging to the Les Saintes fault system (Bazin *et al.* 2010, Feuillet *et al.*, 2011). This mainshock was followed by numerous aftershocks well recorded by the stations of the French Permanent Accelerometric Network.

For this study we selected the M_w=4.5 aftershock that occurred on December 26, 2004 (15h19min) as an Empirical Green's Function (Table 1, Figure 2). Input parameters required to use the simulation code are from Courboulex *et al.* (2010) (Table 2).

It is important to remind that our aim in this study is not to reproduce the ground motions that have been recorded for the mainshock in 2004, but to generate a set of possible source time functions that are variable enough to be representative of a multitude of rupture processes on this fault for a M_w=6.4 earthquakes and then to be representative of the ground motion variability at each site. This was also the aim of Beauval et al. (2009) who tried on the same dataset to test the possibility of using EGF methods for ground motion predictions in probabilistic seismic hazard assessment, but without examining the variability specific to each stations

Simulations are performed on ten different sites of the Guadeloupe archipelago, corresponding to the accelerometric stations of the French Permanent Accelerometric Network that recorded the small earthquakes used as an Empirical Green's Function. These stations are spread throughout the Guadeloupe archipelago, with five stations in Basse-Terre (GHMA, GJYA, PIGA, PRFA and SROA), one station in Grande-Terre (MOLA), three stations in the city of Pointe-à-Pitre (GFEA, GGSA and IPTA) and one station in Marie-Galante Island (GBGA) (Table 3, Figure 2).

A site-specific ground motion variability

For each of the ten stations, we generated 500 simulations of M_w=6.4 earthquakes, and extracted the PGA value for each of. The 500 PGA values picked up were used to build a histogram of the distribution of PGAs for each station (Figure 3). From Figure 3, we can see that the variability of ground motions observed at each site is rather different. To better examine this "site-specific" ground motion variability and remove the effect of distance, we analyzed specifically the results obtained for two different sites of the city of Pointe-à-Pitre, corresponding to IPTA and GGSA accelerometric stations. These two stations were located at approximately the same epicentral distance but on two different soil types (Table 3, Figure 2). IPTA station is on a solid rock and is considered as a good reference station for the city of Pointe-à-Pitre (Lebrun *et al.,* 2004). While the station GGSA is on a swampy soil and is prone to strong site effects. The study of the spectral ratios obtained for the station GGSA, considering IPTA as reference station, showed a strong amplification of ground motions at low frequency with a main resonance frequency observed at 1.15 Hz (Roullé and Bernardie, 2010).

From Figure 4.a and 4.b, the distribution of PGA values seems to follow a lognormal distribution for both stations IPTA and GGSA, while the histograms of the logarithms of PGAs take the form of a normal distribution (Figure 4.c and 4.d). This latter distribution has the advantage of being characterized by a mean value and a standard deviation σ. The validity of the assumption of normality can be verified by testing the fit to the normal distribution of normalized residuals, which are normally distributed with mean 0 and standard deviation 1 (Figure 5.a). In our case, normalized residuals ε is the difference between the values of $\log_{10}(PGA)$ and the mean $\overline{\log_{10}(PGA)}$, normalized by the standard deviation σ:

$$\varepsilon = \frac{\log(PGA) - \overline{\log(PGA)}}{\sigma} \tag{8}$$

The test used to check the hypothesis of normality is graphical method that plots the quantiles of normalized residuals as a function of the quantiles of a theoretical normal distribution with mean 0 and standard deviation 1 (Figure 5.b). The black line represents expected values for this theoretical distribution, while grey crosses represent the values associated with normalized residuals. In Figure 5, which presents the example of station GGSA, we can see that the distribution of normalized residuals showed a good fit to the normal distribution to a level of ±2.5σ. Beyond this value, the distribution of normalized residuals deviated from the normal distribution. In comparison, when the test is performed on the databases used to derive the GMPEs, a similar result is observed: the range of values between which there is generally a good agreement with the normal distribution varies between ±2σ and ±3.5σ (Strasser *et al.,* 2008).

In Figures 4.a and 4.b, we observe that the random variability of ground motions obtained at the station IPTA (on rock) is much smaller than that obtained at the station GGSA (on sediment) which is located at the same epicentral

distance. For the same representation, by taking the logarithm of PGAs (Figure 4.c and 4.d), this variability of ground motions specific to each station is less visible but is still present through the values of standard deviation. Indeed, the station GGSA has a standard deviation σ_{GGSA} = 0.14, which is 1.5 times larger than that of the station IPTA σ_{IPTA} = 0.09. We recall that in our simulation process _the set of source time functions are common for both stations. Therefore, the variability of ground motions observed at each site is not just derived from the variability introduced by different ESTFs.

In Figure 6.a and 6.b we have plotted the accelerograms corresponding to the simulations, which produced respectively the five greatest and the five lowest values of PGA for the station GGSA. Figure 6.c and 6.d represent the same simulations for station IPTA. We observe that the source time functions that generate the extreme values of PGA for the station GGSA are not necessarily those that generate extreme values for the station IPTA. For example, for station GGSA, simulation n°209 (generated with ESTF n°209) produced large values of accelerations and long durations, while the simulation n°142 produces values of accelerations much lower and a PGA seven times smaller. For the station IPTA, simulations n°209 and n°142 are very similar.

Figure 7 shows a little more detail the generation of these simulations in the frequency domain: In Figure 7.a, we can observe that the acceleration Fourier spectrum of the recording at the station GGSA of the small event used as an EGF presents a resonance frequency around 1.2 Hz corresponding to its low-frequency lithological site effect. When this signal is multiplied in the frequency domain by the STF n°209 having a peak at this same frequency, we obtain a simulation with also a very strong peak at this particular frequency. When the same signal is multiplied by the STF n°142, with no peak at this frequency, the simulation obtained did not show either. This has the effect to produce simulations very different in terms of amplitude and duration. In addition, we can see that the acceleration Fourier spectrum of the station on rock IPTA (Figure 7.b) shows no peaks at particular frequencies. So whatever the STF, the simulations obtained are much more similar to each other. Random variability of ground motions at a given site takes therefore its origins in the complexity of the physical processes involved in the generation of ground motion, especially for a station prone to site effects.

Indeed, we have seen that the frequency content of a station with a site effect can sometimes interact with the frequency content of the source to produce extreme values of ground motions. It results in peak values that are prone to be very variable, depending on how the source and site functions interact. For the station on rock, the response of the site will be somewhat more “predictable” providing a variability of ground motion quite small.

Discussion

Both the mean value and the standard deviation are used for the calculation of the probability density functions (PDFs) and the probability curves of exceedance of target levels of acceleration. In Figure 8.a and 8.c, we represent the curves obtained for stations IPTA and GGSA from simulations and we have interpolated the value of acceleration that has a 10% probability of being exceeded at the site if the earthquake occurs. The curves obtained for stations IPTA and GGSA show very different shapes.

Our results are now compared with the ground motion prediction model of Ambraseys *et al.* (2005). This GMPE includes coefficients to account for local site conditions in the calculation of the mean value of ground motion, by using simple site categories based on the shear-wave velocity in the upper 30 m (V_{S30}). However, like most GMPEs, it ignores

any dependence of "sigma" to local site conditions. Although, some studies discuss a possible dependence of standard deviation to magnitude (Abrahamson and Silva, 1997, 2008) or to distance (Blume, 1980; Midorikawa and Ohtake, 2004), there is currently a controversy about the effects of local site conditions on "sigma". If we compare the curves computed for the stations IPTA and GGSA from the GMPE of Ambraseys *et al.* (2005), we can notice that they have shapes quite similar for both stations (Figure 8.b and 8.d).

It is interesting to note also that the standard deviations for the PGA obtained from simulations (respectively 0.14 and 0.09 for stations GGSA and IPTA) are much smaller than that obtained from the model of Ambraseys *et al.* (2005), which is equal to 0.26. Typical values of standard deviation of recent GMPEs are 0.2 to 0.3 for the PGA (Douglas, 2003). This can be easily explained by the fact that, unlike GMPEs, our study considers a source-site configuration very simplified with only one fault Recent studies for different tectonic regions (e.g. Atkinson, 2006; Morikawa *et al.*, 2008; Lin *et al.*, 2011) show that considering a single source of earthquakes, the standard deviation of ground motions recorded at a single station is much lower than that obtained by regression analyses of ground motion data coming from many different sites and including several seismic sources, as in GMPEs. However, GMPEs are used to predict site-specific ground motions assuming that the variability predicted by the database is comparable to the variability of ground motions at a single site over time. This is the ergodicity assumption (Anderson and Brune, 1999). This could be partially responsible for values of standard deviation that would incorporate a variability of ground motion potentially greater than it can be physically justified.

Since the standard deviations obtained from our simulations and the GMPE of Ambraseys *et al.* (2005) do not contain fully the same information, it is more interesting to study them in absolute. Thus, Figure 8 highlights the involvement of a site-specific standard deviation value to compute the probability of exceedance of a target level of acceleration at a site. While the simulations provide a variability of ground motions specific to each site, the GMPEs, despite equations more and more complex to account for additional site information (Douglas *et al.*, 2009), consider the same variability of ground motions whatever the site conditions. This has the effect of producing results with little distinction between a site on rock and a site on sedimentary soil, and probably a less realistic consideration of site effects.

Conclusion

In this study, we analyzed the ground motion variability that can be generated at a given site from a database of synthetic accelerograms. By using the Empirical Green's Function method, we generated 500 different simulations of M_w=6.4 earthquakes occurring on the fault at the origin of the Les Saintes earthquake (Guadeloupe) of November 21, 2004.

The main result is that we obtained a site specific ground motion variability. By studying in detail the example of two stations located in the city of Pointe-à-Pitre, we observed that the variability of ground motions obtained at the station on rock IPTA is much smaller than that obtained at the station on soft soil GGSA located at the same epicentral distance. Random variability of ground motions at a given site seems to originate from the complexity of the physical processes involved in the generation of ground motions. Especially for a station subject to site effects, for which the combined effects of the seismic source and site properties can produce very high accelerations. However, most GMPEs

used in seismic hazard analysis ignore any dependence of "sigma" to local site conditions, leading to a less realistic consideration of site effects in probabilistic calculations. It should thus verify on actual database if some sites may really cover a variability of ground motions larger than others. This future study could be carried out in regions of the world with enough ground motion records at individual sites for a single source region of earthquakes. But the number of databases permitting such studies is still rather limited.

References

Abrahamson, N.A., and W.J. Silva (1997). Empirical response spectral attenuation relations for shallow crustal earthquakes, *Seismol Res. Lett.* **68**, 94-127, doi: 10.1785/gssrl.68.1.94.

Abrahamson, N.A., and W.J. Silva (2008). Summary of the Abrahamson and Silva NGA ground motion relations. *Earthquake Spectra* **24**, 67-97.

Aki, K. (1967). Scaling law of seismic spectrum, *J. Geophys. Res.* **72**, 1217-1231.

Al Atik, L., N. Abrahamson, J.J. Bommer, F. Scherbaum, F. Cotton, and N. Kuehn (2010). The variability of ground-motion prediction models and its components, *Seismol. Res. Lett.* **81**, 794-801, doi: 10.1785/gssrl.81.5.794.

Ambraseys, N. N., J. Douglas, S. K. Sarma, and P. M. Smit (2005). Equations for the estimation of strong ground motions from shallow crustal earthquakes using data from Europe and the Middle East: horizontal peak ground acceleration and spectral acceleration, *Bull. Earthq. Eng.* **3**, 1-53.

Anderson, J. G., and J. N. Brune (1999). Probabilistic seismic hazard analysis without the ergodic assumption, *Seims. Res. Lett.***70**, 19-28.

Atkinson, G. M. (2006). Single-station sigma, *Bull. Seism. Soc. Am.*, **96**, 446-455.

Bazin, S., N. Feuillet, C. Duclos, W. Crawford, A. Nercessian, M. Bengoubou-Valérius, F. Beauducel, and S. C. Singh (2010). The 2004–2005 Les Saintes (French West Indies) seismic aftershock sequence observed with ocean bottom seismometers, *Tectonophysics*, 489(1-4), 91-103.

Beauval, C., L. Honoré, and F. Courboulex (2009). Ground-Motion Variability and Implementation of a Probabilistic-Deterministic Hazard Method, *Bull. Seis. Soc. Am*, 99(5), 2992-3002.

Bertil, D., S. Bès de Berc, and J. Douglas (2005). Synthèse de la crise sismique des Saintes (Guadeloupe) entre le 21 novembre 2004 et le 30 mars 2005, Rapport BRGM/RP-54401-FR.

Blume, J.A. (1980). Distance partitioning in attenuation studies. Proceedings of the 7th World Conference on Earthquake Engineering, **2**, 403-410.

Bommer, J.J., and N.A. Abrahamson (2006). Why do modern probabilistic seismic-hazard analyses often lead to increased hazard estimates ?, *Bull. Seism. Soc. Am.* **96**, 1967-1977, doi : 10.1785/0120060043.

Brune, J.N. (1970). Tectonic stress and the spectra of seismic shear waves from earthquakes, *J. Geophys. Res.* **75**, 4997-5009.

Courboulex, F., J. Converset, J. Balestra, and B. Delouis (2010). Ground-motion simulations of the 2004 Mw6.4 Les Saintes, Guadeloupe, earthquake using ten smaller events, Bull. Seism. Soc. Am. 100, 116-130.

Douglas, J. (2003). Earthquake ground motion estimation using strong-motion records: a review of equations for the estimation of peak ground acceleration and response spectral ordinates, *Earth-Science Reviews* **61**, 43-104.

Douglas, J., P. Gehl, L.F. Bonilla, O. Scotti, J. Régnier, A-M. Duval, and E. Bertrand (2009). Making the most of available site information for Empirical Ground-Motion Prediction, *Bull. Seism. Soc. Am*. **99**, 1502-1520, doi: 10.1785/0120080075.

Feuillet, N., F. Beauducel, E. Jacques, P. Tapponnier, B. Delouis, S. Bazin, M. Vallée, and G. C. P. King (2011), The Mw = 6.3, November 21, 2004, Les Saintes earthquake (Guadeloupe): Tectonic setting, slip model and static stress changes, *J. Geophys. Res.*, 116, B10301, doi:10.1029/2011JB008310.

Hartzell, S. H. (1978). Earthquake aftershocks as Green's functions, *Geophys. Res. Lett.* **5**, 1-4.

Hiemer, S., F. Scherbaum, D. Roessler, and N. Kuehn (2011). Determination of τ_0 and rock site k from records of the 2008/2009 earthquake swarm in western bohemia, *Seism. Res. Lett.* **82**, 387-393.

Joyner, W. B., and D. M. Boore (1986). On simulating large earthquakes by Green's function addition of smaller earthquakes, *American Geophysical Union Monograph* **37**, 269-274.

Kohrs-Sansorny, C., F. Courboulex, M. Bour, and A. Deschamps (2005). A two-stage method for ground-motion simulation using stochastic summation of small earthquakes, *Bull. Seism. Soc. Am.* **95**, 1387-1400.

LeBrun, B., A-M. Duval, P-Y. Bard, O. Monge, M. Bour, S. Vidal, et al. (2004). Seismic microzoning: a comparison between geotechnical and seismological approaches in Pointe-à-Pitre (French Western Indies), *Bull. Earthquake Eng.* **2**, 27-50.

Lin, P., B. Chiou, N. Abrahamson, M. Walling, C.-T. Lee, and C. Cheng (2011). Repeatable source, site and path effects on the standard deviation for empirical ground-motion prediction models, *Bull. Seismol. Soc. Am.* (in press).

Midorikawa, S., and Y. Ohtake (2004). Variance of peak ground acceleration and velocity in attenuation relationships. Proceedings of the 13th World Conference on Earthquake Engineering, Vancouver, Paper n° 325.

Morikawa, N., T. Kanno, A. Narita, H. Fujiwara, T. Okumura, Y. Fukushima, and A. Guerpinar (2008). Strong motion uncertainty determined from observed records by dense network in Japan, *J. Seismol.* **12**, 529-546.

Ordaz, M., J. Arboleta, and S. K. Singh (1995). A scheme of random summation of an empirical Green's function to estimate ground motions from future large earthquakes, *Bull. Seism. Soc. Am.* **85**, 1635-1647.

Pequegnat, C., P. Guéguen, D. Hatzfeld, and M. Langlais (2008). The French Accelerometric Network (RAP) and National Data Center (RAP-NDC), *Seismol. Res. Lett.* **79**, 79-89.

Reiter, L. (1990). Earthquake Hazard Analysis: Issues and Insights, Columbia University Press, New York, 254 pp.

Rodriguez-Marek, A., G.A. Montalva, F. Cotton, and F. Bonilla (2011). Analysis of songle-station standard deviation using the KiK-net data, *Bull. Seism. Soc. Am.* **101**, 1242-1258, doi: 10.1785/0120100252.

Roullé, A., and S. Bernardie (2010). Comparison of 1D non-linear simulations to strong-motion observations : a case study in a swampy site of French Antilles (Pointe-à-Pitre, Guadeloupe), *Soil Dyn. Earthq. Eng.* **30**, 286-298.

Strasser, F.O., J.J. Bommer, and N.A. Abrahamson (2008). Truncation of the distribution of ground-motion residuals, *J. Seismol.* **12**, 79-105, doi: 10.1007/s10950-007-9073-z.

Wennerberg, L. (1990). Stochastic summation of empirical Green's functions, *Bull. Seism. Soc. Am.* **80**, 1418-1432.

TABLES

Table 1

Parameters of the aftershock used as an Empirical Green's Function in the simulation method (from Courboulex et al, 2010).

Date	Hour	M_w	Latitude (°)	Longitude (°)	Depth (km)	Focal mechanism strike (°)/dip (°)/rake (°)
2004/12/26	15h19m15s	4.5	15.7477	-61.5773	10.5	135 / 35 / -95

Table 2

Input parameters for the simulation of an M_w=6.4 earthquake by using the M_w=4.5 aftershock of December 26, 2004 (15h19) as an Empirical Green's Function (Courboulex *et al.,* 2010).

C	*N*	M_w target event	F_c target event (Hz)	m_w EGF	f_c EGF (Hz)
11.	4	6.4	0.12	4.5	0.48

Table 3

Location and local site geology of the accelerometric stations used in this study (French Permanent Accelerometric Network; see: http://www-rap.obs.ujf-grenoble.fr) and epicentral distances to the aftershock of December 26, 2004 (15h19).

Station code	Locality	Latitude (°)	Longitude (°)	Local site geology	Epicentral distance (km)
GBGA	Marie Galante – Grand Bourg	15.883	-61.317	Rock	32
GFEA	Pointe-à-Pitre – Ecole Fengarol	16.240	-61.537	Sediment	55
GGSA	Abymes - Aéroport Glide	16.266	-61.542	Sediment	57
GHMA	Houëlmont Gourbeyre	15.981	-61.704	Rock + Topographic site effect	29
GJYA	Saint Claude - Belfond	16.014	-61.705	Rock	32
IPTA	Pointe-à-Pitre - Institut Pasteur	16.233	-61.528	Rock	54
MOLA	Météo Le Moule - Radar	16.315	-61.349	Rock	67
PIGA	Bouillante – Ecole Pigeon	16.147	-61.769	Rock	48
PRFA	Basse Terre - Préfecture	15.992	-61.722	Rock	31
SROA	Sainte Rose - Lycée	16.332	-61.707	Sediment	66

FIGURES

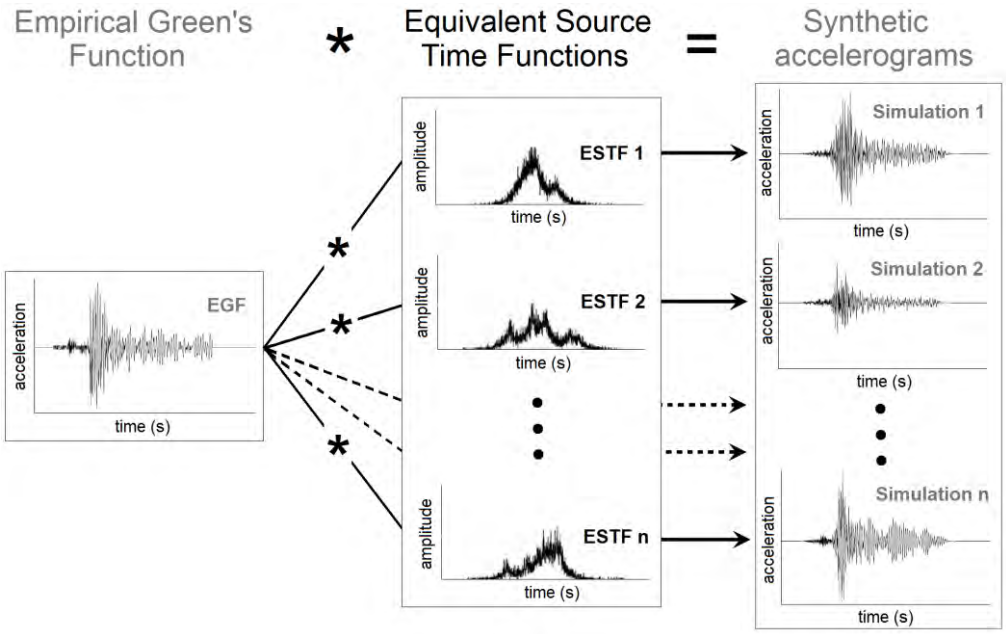

Figure 1. Principle of the simulation method used in this study: synthetic accelerograms of the target event are obtained from the convolution product between the small-event record taken as an Empirical Green's Function and Equivalent Source Time Functions (ESTFs).

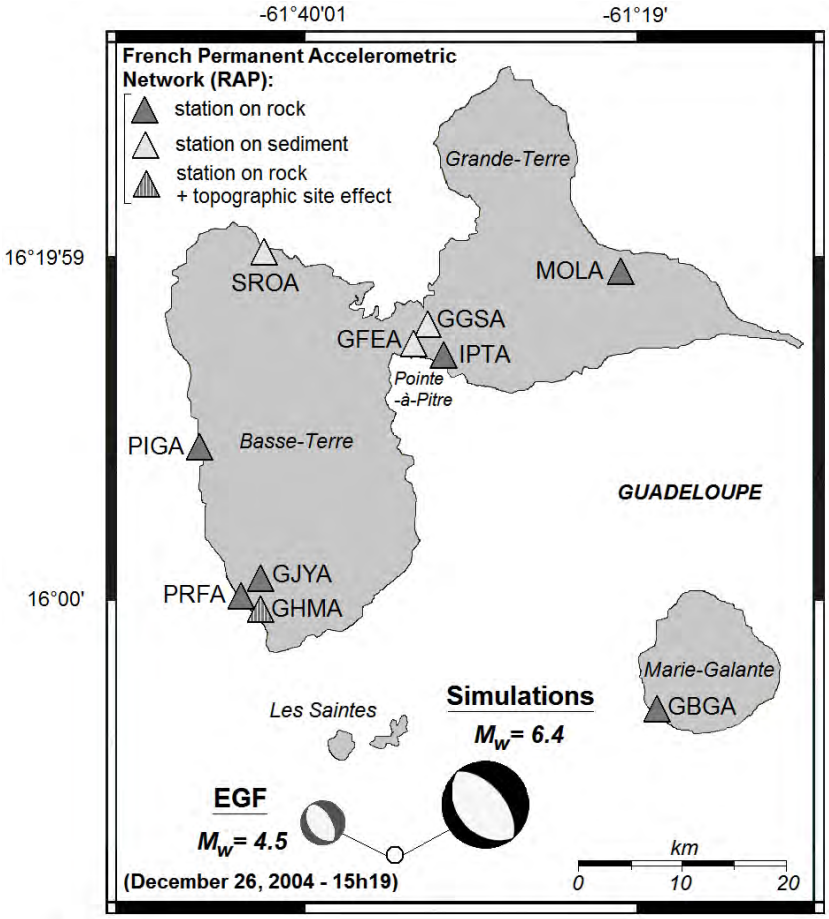

Figure 2. Epicenter and focal mechanism of the M_w=4.5 earthquake (December 26, 2004 - 15h19) taken as an Empirical Green's Function for the simulation of M_w=6.4 earthquakes, and location of the accelerometric stations used in this study (French Permanent Accelerometric Network).

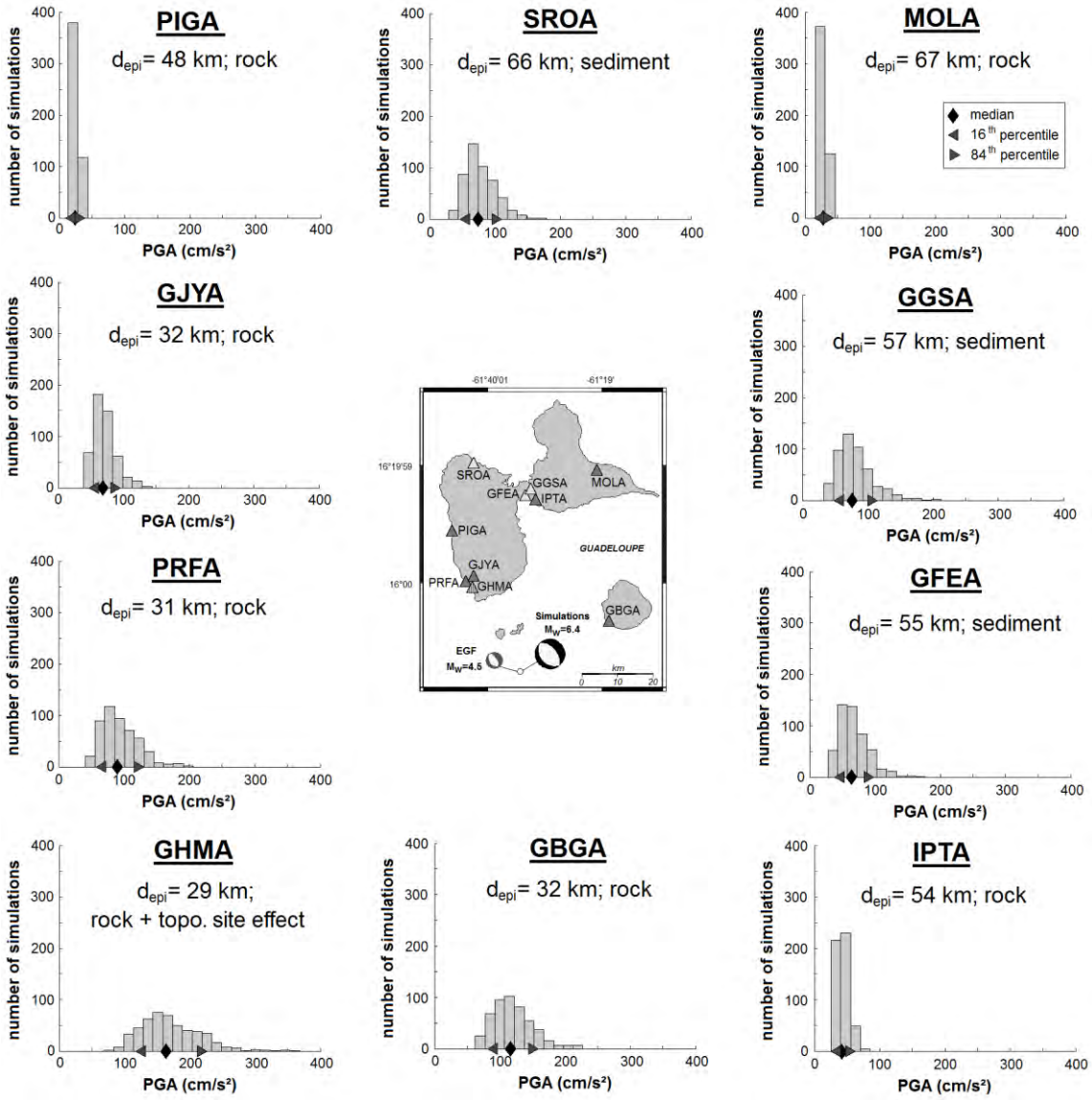

Figure 3. Histograms of the distribution of PGA values obtained from 500 simulations of M_w=6.4 earthquakes for each of the ten stations (eastern component).

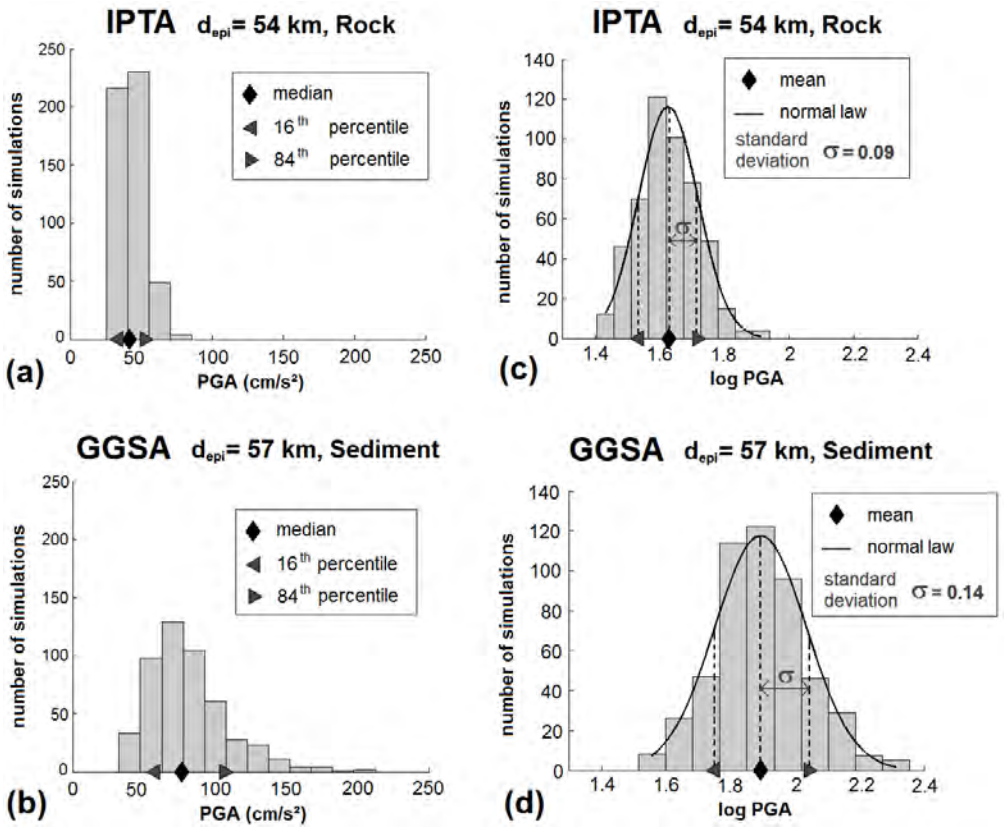

Figure 4. (a)(b) Histograms of the distribution of PGA values obtained from 500 simulations of M_w6.4 earthquakes for stations IPTA (Rock, $d_{épi}$ = 54 km) and GGSA (Sediment, $d_{épi}$ = 57 km); (c)(d) Histograms of the distribution of $\log_{10}$(PGA) values for stations IPTA and GGSA (eastern component).

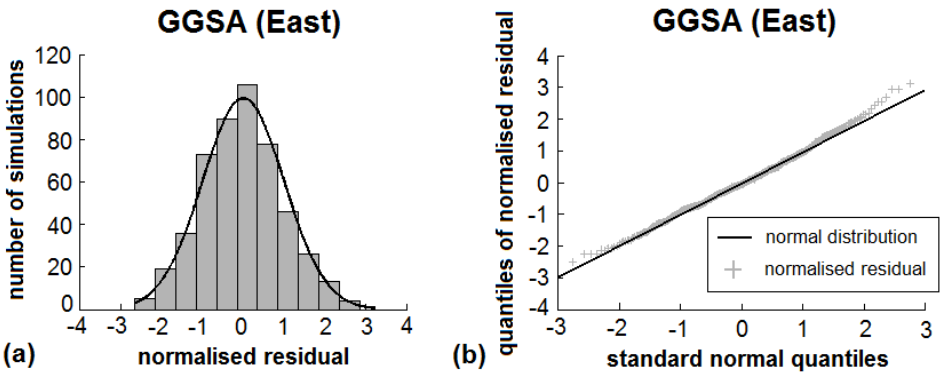

Figure 5. (a) Histogram of normalized residuals for station GGSA (eastern component) and associated normal distribution with mean 0 and standard deviation 1; (b) Quantile-quantile test of fit to the normal distribution of normalised residuals for station GGSA (eastern component).

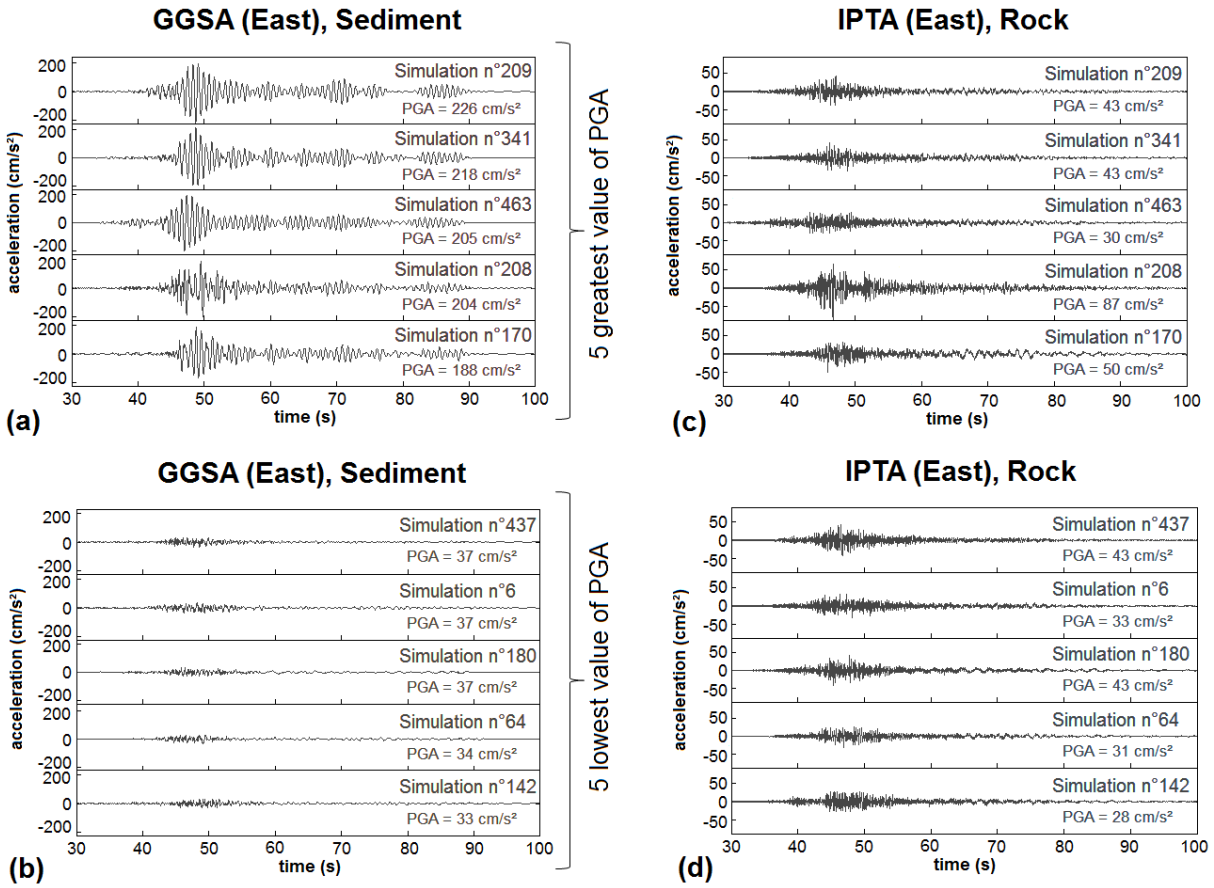

Figure 6. Synthetic accelerograms of the simulations producing (a) the five greatest values of PGA and (b) the five lowest values of PGA for the station GGSA (eastern component); (c)(d) corresponding simulations for the station IPTA (eastern component).

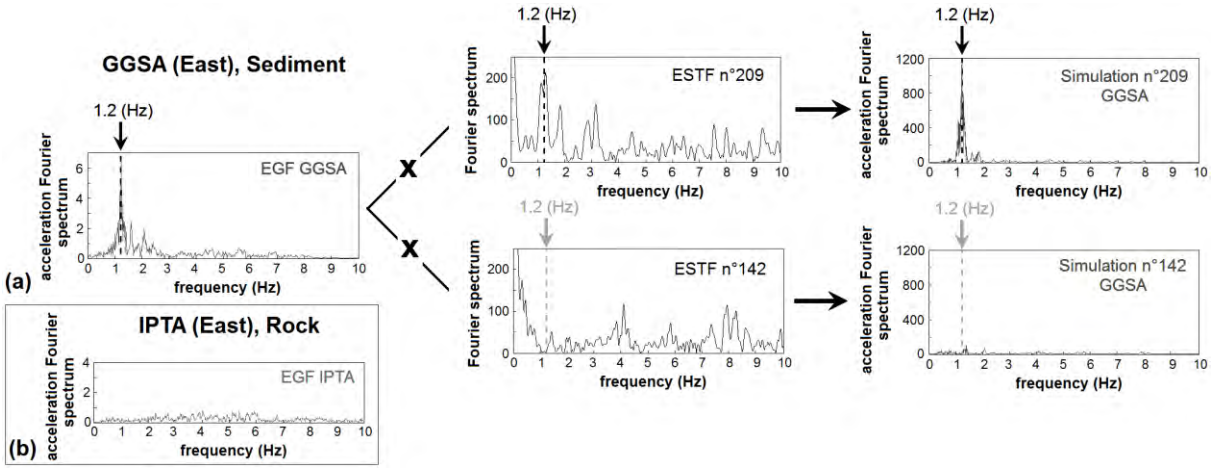

Figure 7. (a) Acceleration Fourier spectra of simulations n°209 and n°142 at the station GGSA (eastern component) obtained respectively from the ESTFs n°209 and n°142 and the acceleration Fourier spectrum of the small event used as an EGF; (b) Acceleration Fourier spectrum for the station IPTA (eastern component).

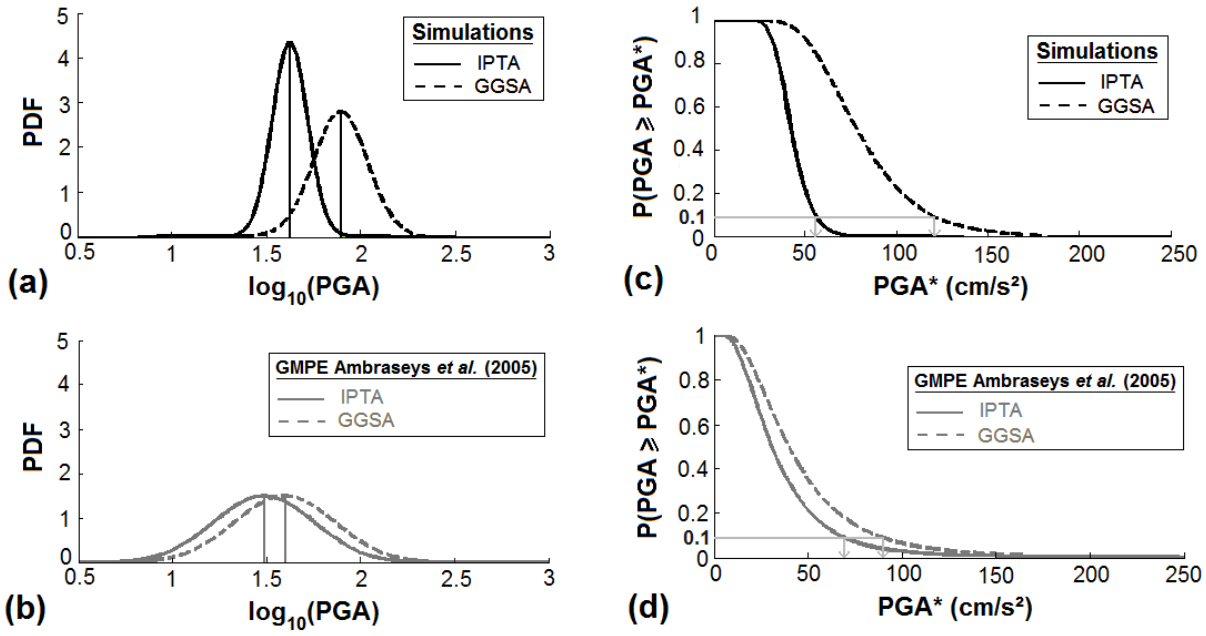

Figure 8. (a)(b) Probability density functions for stations IPTA and GGSA from simulations and from the GMPE of Ambraseys *et al.* (2005); (c)(d) Probability curves of exceedance of target levels PGA* computed for stations IPTA and GGSA from simulations and from the GMPE of Ambraseys *et al.* (2005) and acceleration values (grey arrows) having a probability of 10% to be exceed at a site if the earthquake occurs.